Journal of Materials and Environmental Science
ISSN : 2028-2508
e-ISSN : 2737-890X
CODEN : JMESCN

J. Mater. Environ. Sci., 2022, Volume 13, Issue 05, Page 526-543

http://www.jmaterenvironsci.com

Adsorption of Congo Red onto Organo-Modified Bentonite: kinetic, equilibrium and thermodynamic studies

A. Oussalah[1], A. Aichour[2], A. Hellati[3], A. Boukerroui*[1]

[1]*LTMGP Laboratory, Chemistry Department, Faculty of Exact Sciences, University of Bejaia, 06000 Bejaia, Algeria.*
[2] *LCEP Laboratory, Department of Engineering Processes, Faculty of Technology, University of Setif-1, Setif, Algeria.*
[3]*LPMAMPM Laboratory, University of Bord Bou Arreridj 34000 Algeria*

**Corresponding author, Email address: abdelhamid.boukerroui@univ-bejaia.dz*

Received 29 June 2021,
Revised 09 May 2022,
Accepted 10 May 2022

Keywords
- ✓ Organobentonite
- ✓ Congo red,
- ✓ Calcium alginate
- ✓ adsorption,
- ✓ Isotherms
- ✓ Kinetic

abdelhamid.boukerroui@univ-bejaia.dz
Phone: (+213)662701867

Abstract

In the present paper, a natural bentonite (B) has been modified with a cationic surfactant hexadecyltrimethylammonium bromide (OB) and then encapsulated into calcium alginate to prepare a novel organobentonite composite beads (A-OB), in order to remove a Congo Red (CR) dye from aqueous solution, using a batch adsorption process. The A-OB beads were characterized using FTIR, SEM, and pH_{PZC} analysis. The performance of the obtained composite beads through the removal of the CR dye was evaluated by the effect of the following parameters: initial dye concentration (25-300 mg L^{-1}), contact time (5-1700 min) and temperature (10-40 °C). A kinetic study indicated that adsorption was governed by the pseudo-second order kinetic equation and that the adsorption process is best described by Langmuir isotherm model. The results showed that the maximum adsorption capacity (q_{max}) of A-OB composite beads was 218 mg g^{-1}. Furthermore, thermodynamic studies showed spontaneous and exothermic nature of the overall adsorption process. The regeneration study confirmed that the present composite beads can be regenerated up to fifth cycle successfully. The results indicate that alginate-organobentonite composite beads are efficient adsorbents and could be used as a low-cost material for the removal of Congo Red anionic dyes from wastewater.

1. Introduction

There are different classes of dyes used by many industries to color their products. These dyeing processes require a substantial amount of water and generate large volumes of coloured wastewaters. It is known toxic dyes present in this wastewater degrade the ecosystem [1]. To stop this environmental pollution, dyes must be removed from wastewater before they are discharged into waterways. Anionic azo dyes, such as Congo red (CR), are known to have the potential to bioaccumulate, metabolise into carcinogens and cause allergy problems. Congo red is an electrophilic dye that is extremely toxic to the living body [1,2]. Various techniques for removing dyes include physicochemical, chemical and biological methods, such as bioassays coagulation and flocculation, precipitation, ion exchange, membrane filtration, electrochemical destruction, irradiation, ozonation and adsorption [1,3-5]. Among these methods, comparatively, adsorption process is a very effective separation technique, due to its convenience, ease of use and simplicity of design [5-7].

Several solid materials, can be used as adsorbents for dyes in aqueous solution [5-9]. Among these adsorbents, bentonite clays which are abundant and low-cost adsorbents have a strong affinity for the removal of dyes present in an aqueous solution [5;8;10;11]. According to the literature, the adsorption

capacity of clays is commonly high for cationic dyes, while a low adsorption capacity has been obtained for anionic dyes [5;12]. The reason for this case is that the negative surface charges of clays, due to isomorphic substitutions, allow the adsorption of anionic dyes (e.g., Congo red) in very small quantities [12-14]. Hence, the surface of natural clays must be modified in order to improve their adsorption capacities for anionic dyes [15,16]. In this study, the surface of clay was modified with a cationic surfactant [17]. Indeed, many reports showed that the hexadecyl trimethyl-ammonium bromide (HDTMAB) surfactant -used as a modifying agent- displayed higher adsorption capacity than the original clay and that the resulting organoclay material might be an ideal multifunctional adsorbent for various types of contaminants, such as the CR dye [10,15,18,19].The use of organobentonite as an adsorbent is great interest, due to its efficiency, cost, abundance and exhibits strong affinities for Congo red adsorption [20].

Recently, to improve the adsorption capacity of bentonite, some problems have arisen such as the difficulty in separating the solid matter from the treated water. To avoid problems of liquid-adsorbent separation at the end of the adsorption process, great interest is focused on the use of mixed alginate/material composite beads such as bentonite/natural alginate composite beads [12,21,22], alginate-nano-goethite beads [23] and alginate/regenerated spent bleaching earth [9].

In this study a new adsorbent was synthesized from modified bentonite clay using hexadecyl trimethyl-ammonium bromide as a modifying agent and a natural polymer namely alginate. The adsorption capability of the synthesized beads was tested for removal of Congo red (CR). The main objectives of the present study are to investigate the adsorption mechanism of CR onto alginate-organobentonite composite beads, by using several parameters having an effect on the batch adsorption process (pH, contact time, initial concentration and temperature effects). Also, adsorption isotherms, kinetics and thermodynamic parameters were investigated. It is a contribution to improvement adsorptive capacities of organo-modified bentonite in the removal of anionic dye.

2. Methodology

2.1 Material

Raw bentonite (denoted "B") originating from Maghnia deposit (Western of Algeria) was kindly offered by Bental Company (Algeria). The natural bentonite was grounded and sieved into fractions using ASTM standard sieves, and particle sizes of 60-100 µm were used in the experiments. Chemical analysis of B yielded the following data: 69.4% SiO_2, 14.7% Al_2O_3, 1.1% MgO, 0.8% K_2O, 0,3% CaO, 1.2% F_2O_3, 0.5% Na_2O, 0.2% TiO_2, 0.05% As, and a loss on ignition of 11% [24]. These results indicate that silica and alumina are the major constituents of bentonite. The SiO_2 /Al_2O_3 ratio (4.7) is higher than the conventional value of bentonite (about 2.7), due to the presence of free silica (quartz) in the clay fraction [25]. In addition, the mineralogical analysis has shown that the raw bentonite contains mainly montmorillonite (86 wt %); the bentonite composition also includes as impurity; quartz, cristobalite and beidellite [24, 26]. The cationic exchange capacity (CEC) of B determined by the methylene blue method was 91 meq/100 g [24, 27], and the BET specific surface area (obtained with a Micromeritics ASAP 2020) was equal to 84 m^2/ g [12,24]. After grinding and sieving, B samples were used as precursor for the preparation of the organo-modified bentonite. The hexadecyl trimethyl-ammonium bromide (HDTMAB), sodium alginate, hydrochloric acid, calcium chloride, sodium hydroxide and Congo red (chemical formula: $C_{32}H_{22}N_6Na_2O_6S_2$ abbreviated as CR, molecular weight: 696,663 $g.mol^{-1}$, λ_{max} = 541 nm) were purchased from Sigma-Aldrich Chemicals and used without any purification. Distilled water was used for the preparation of all required solutions. The pH of solutions was measured by a pH-meter (Hanna 2210) equipped with a combined glass electrode.

2.2 Preparation of organobentonite

A suspension of bentonite (B) was treated by adding amounts of the cationic surfactant equivalent to 100 % of the CEC value of B. The amount of surfactant was dissolved in distilled water and a mass of 10 g of bentonite was added to the surfactant solution under stirring for 3h at 80 °C. The separated samples were washed with distilled water several times, until the bromide ions had completely disappeared and then dried at 80 °C. The material obtained was named OB. Organo-modified bentonite composite beads were prepared by encapsulation within calcium alginate using the same method reported in our previous works [8,9,12,22]. A solution of 2% (w/v) sodium alginate was previously prepared by stirring for 4 h, then 2 g of organobentonite (OB) have been added to it. The mixture was stirred for 24 h and dropped through a syringe into a calcium chloride solution (4% w/v) to form a composite material of calcium alginate/organobentonite beads. Beads were washed several times with distilled water, then dried for 48 h at room temperature and stored in a clean bottle. The composite beads were named A-OB.

2.3 Characterization of prepared samples

The infrared spectra of organo-modified bentonite (OB), calcium alginate (A) and calcium alginate/organobentonite composite beads (A-OB) were analyzed using Fourier Transform Infrared spectroscopy (FTIR) (Perkin-Elmer spectrum FT-IR model 65 spectrometer) in the range of 4000-400 cm^{-1} with KBr pellet technique. Scanning Electron Microscopy (SEM) analyses were performed using a CARL ZEISS GEMINI high resolution field emulation scanning electron microscope (FESEM). The determination of point of zero charge (pH_{PZC}) of A-OB composite beads was performed according to the batch equilibrium method. Initial pH values (pH_i) of 0.01M NaCl solutions (50 mL) were adjusted to a pH range of 2-12 using 0.1M HCl or NaOH. Then 0.2 g of adsorbent was added to each sample. Suspensions were stirred for 48 h at room temperature (24°C), filtered and the final pH of solutions (pH_f) was measured. The point of zero charge (pH_{PZC}) was obtained from the plot of (pH_i-pH_f) versus pH_i.

2.4 Batch adsorption study

The adsorption of Congo red (CR) was conducted in a batch system. All mixtures were stirred at room temperature (23-25 °C) and under a natural pH of Congo red solutions (6.5-8.5). CR adsorption isotherm onto A-OB was investigated using a range of initial concentration from 25 to 800 mg L^{-1}. A mass of adsorbent equal to 10 mg was added to a volume of 10 mL of each initial dye concentration. Solutions were shacked until equilibrium time, and then analyzed at 541 nm using UV-VIS spectrophotometer (Optizen 3220 UV apparatus). The adsorption capacity of CR on the adsorbent at equilibrium was calculated using **Eqn. 1**.

$$q_e = \frac{(C_0 - C_e)V}{m} \qquad \textbf{Eqn. 1}$$

Where C_o and C_e are the initial and equilibrium concentrations (mg L^{-1}) of CR solutions, respectively, V is the volume of the working solution (L), and m is the weight (g) of adsorbent used. Each experiment was repeated three times and the mean values were considered in the fitting process.

2.2 Kinetic study

The kinetic experiments were carried out at room temperature (24±1 °C) and at natural pH of CR solutions (pH_{CR}= 6.5-7.5) in the batch system. For each experiment, 100 mL of the CR dye solution at specified concentrations (25, 50, 100, 200 and 300 mg L^{-1}) were continuously stirred with 0.1g of A-OB

composite during different time intervals (1-480 min). At each contact time a sample of CR dye was taken and analyzed using UV-visible spectrophotometer at 541 nm wavelength. The amount of CR adsorbed (mg) per unit mass of adsorbent (g) at time t (min) named q_t (mg g^{-1}) was calculated by using **Eqn. 2**:

$$q_t = \frac{(C_0 - C_t)V}{m} \qquad \textbf{Eqn. 2}$$

Where C_t (mg L^{-1}) is the liquid-phase concentration of CR at time t.

2.6 Effect of temperature

The effect of temperature on the adsorption of the CR dye on A-OB was also investigated in order to find out the nature of the process by using an initial concentration of 100 mg L^{-1} at natural pH of dyes and at different temperatures (10, 20, 30 and 40 °C); a volume of 10 mL was added to 10 mg of adsorbent A-OB. Dye solutions were stirred to equilibrium time, and then analyzed in the UV-Vis [12]. The adsorbed amount was calculated using **Eqn. 1** as described above.

2.3 Regeneration study

The reusability of an adsorbent is a potential parameter; which make its use in the field of wastewater treatment efficient. CR desorption from the composite A-OB was investigated using distilled water at pH 10 as desorbing agent. Indeed, it was observed by some authors that a very highly basic pH leads to a better desorption of the dye and the CR dye changes its original red color beyond a pH of 10 [28,29, 33,37]. Desorption experiments were carried out by agitating for 48 h at room temperature, using 100 mL of desorbing agent and 100 mg of A-OB composite, saturated with CR dye (100 mg L^{-1}). After desorption A-OB composites were washed several times with distilled water until neutrality, dried at room temperature and reused for five cycles of adsorption-desorption experiments (pH_{CR} = 7.2, T = 24°C, v_{agit} = 200 rpm) [12]. CR removal for a cycle of regeneration R (%) was calculated by using the following equation (**Eqn. 3**):

$$R(\%) = \frac{q_{des}}{q_{ads}} \times 100 \qquad \textbf{Eqn. 3}$$

Where q_{ads}, q_{des} are the amounts of adsorbed and desorbed dyes respectively (mg g^{-1}).

3. Results and Discussion

3.1 Characterization by FTIR spectroscopy

The FTIR spectra of alginate (A), organobentonite (OB), alginate-organobentonite beads (A-OB) are shown in **Figure 1**. It's well known, that the broad peak between 3300 and 3650 cm^{-1} is due to stretching vibration of OH (A, OB, and A-OB spectrum). This band is typical of the adsorption of water by clay, alginate and organoclays [30]. The sharp band at 3624 cm^{-1} is associated to the Al-OH and Mg-OH vibrations. The peak at 1638 cm^{-1} is attributed to the bending vibration of the physically adsorbed water, while the peak at 1029 cm^{-1} is due to the Si-O stretching vibrations, which is also mainly associated with montmorillonitic clays [31]. FTIR spectrum of alginate (A) shows absorption band at 2924 cm^{-1} assigned to the –CH stretching vibration. The bands at 1619 and 1412 cm^{-1} are attributed to the OH of H_2O bending band and COO^- antisymmetric stretching respectively [32]. In addition, a pair of new bands appeared at 2850 and 2923 cm^{-1} (OB, A-OB), which can be assigned to the symmetric and antisymmetric stretching vibrations of the methylene group [30]. These observed peaks confirm the intercalation of the cationic surfactant into the interlayer gallery of the bentonite [33].

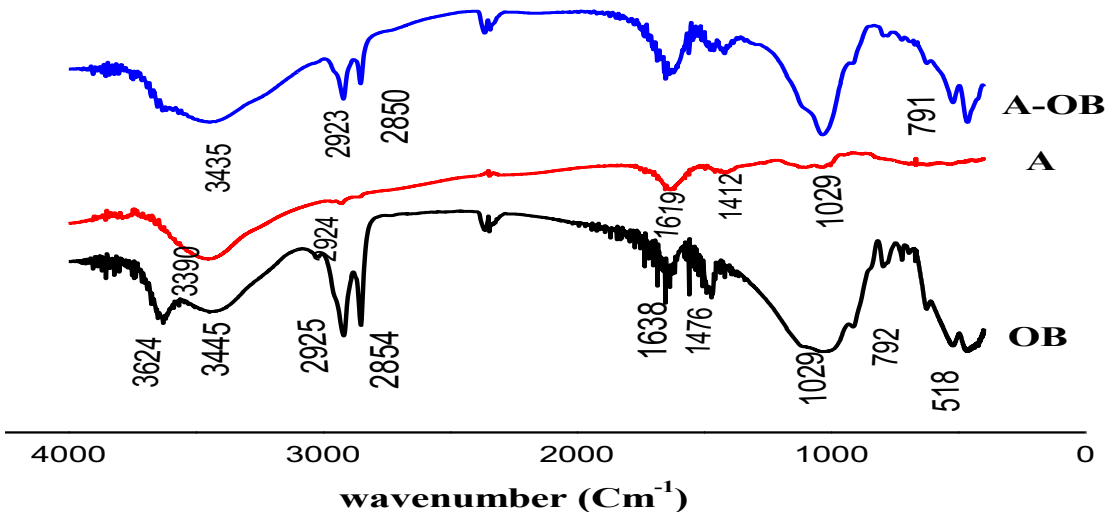

Figure 1. FTIR spectra of organobentonite (OB), Alginate (A), and alginate-organobentonite composite beads (A-OB)

The FTIR spectra in **Figure 1** presented all the characteristics of bentonite and alginate and do not show any changes.

3.2 Characterization by Scanning Electron Microscopy (SEM)

The morphological features of A-OB composite beads were obtained by SEM and presented in **Figure 2**.

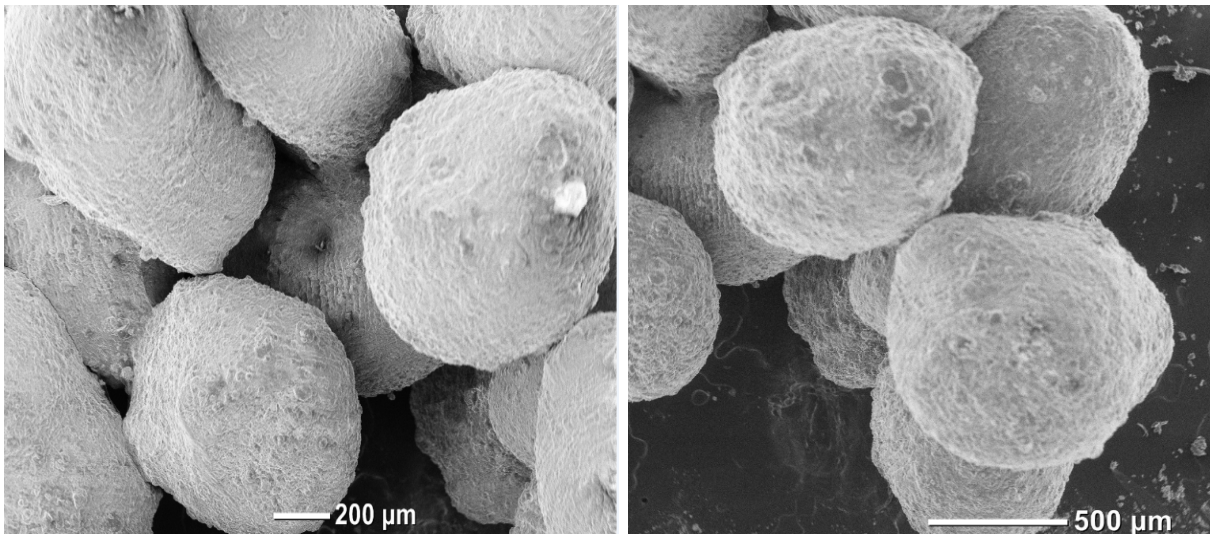

Figure 2. SEM images of A-OB at 500 µm and 200 µm resolution

The samples have shown a rough and heterogeneous surface structure, and small pores are present on their surface due to the presence of clay in the composite beads [34].

3.4 Point of zero charge (pH_{PZC}) and pH effect

Congo red is a dipolar molecular. It exists as anionic form at basic pH (pH>5.5) and as cationic form at acidic pH (pH<5.5) [19,28]. For the interpretation of the effect of pH on the CR adsorption, the point of zero charge (pHpzc) of adsorbent must be investigated.

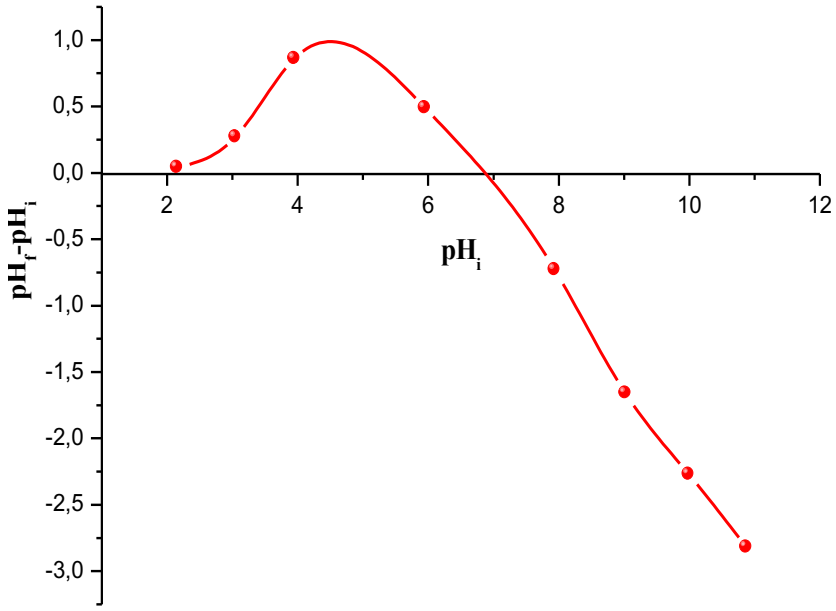

Figure 3. pH_{PZC} of A-OB

The results presented in **Figure 3** show that the adsorbent has zero potential charge at its surface at pHpzc, has a positively charged surface at pH <pHpzc, and has a negatively charged surface at pH>pHpzc. The pHpzc= 6.6 value is very close to the pH of CR solutions (6.5-7.5) and similar results are also reported elsewhere [29,36-38]. The effect of pH on CR adsorption was studied in a pH range of 4-12 and the results are shown in **Figure 4**.

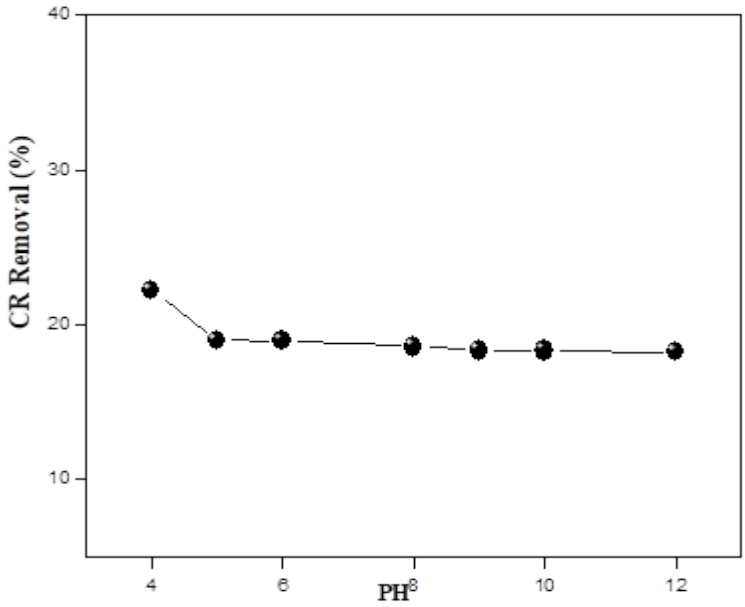

Figure 4. Effect of pH on the CR adsorption onto A-OB (initial concentration =100 mg L^{-1}, m=10 mg, T = 24 ± 1°C)

The highest CR removal percent was found at pH 4. It decreases from 22.21 % to 18.23 % with the increase of pH from 4 to 12. However, it can be notice that the removal percent values have relatively stabilized after pH 5.

The positively or negatively charged active sites to the adsorbent surface (see **Figure 3**) do not favour the removal of CR at acid and basic pH respectively. This is may be due to the competition of H^+ with CR ions (in its cationic form) for the cationic sites of the composite. While in basic medium, this is may be due to the competition of OH^- ions with CR ions (in its anionic form) for the anionic active sites of the composite [12,33,38]. Because of this, the surface charge of adsorbent is likely to be Si-OH_2^+, Al-OH_2^+, and Si-O^- , Al-O^- in acidic and alkaline medium, respectively [39].

the most of studied aqueous solutions have a pH between 6.5 and 7.5, maintaining the natural pH of the solution (6.5–7.5), close to pHpzc, without adjustment, has environmental and economic advantages. In fact, the treated water can be discharged directly to watercourse without a need to add additional reagents to adjust its pH. The system is easy to maintain, and it can be applied at an industrial scale in a cost-effective manner. For our future experiments, we have chosen to work without any adjustment of the pH of solutions.

3.4 Kinetic study

In order to evaluate the kinetic behavior of the adsorbent, two kinetic models -pseudo-first-order (PFO; **Eqn. 4**) and pseudo-second-order (PSO; **Eqn. 5**) models- were applied to the experimental data:

$$Log(q_e - q_t) = logq_e - \frac{k_1}{2.303}t \qquad \textbf{Eqn. 4}$$

$$\frac{t}{q_t} = \frac{1}{k_2 q_e^2} + \frac{1}{q_e}t \qquad \textbf{Eqn. 5}$$

With $h = k_2 q_e^2$

Where t is the time (min) and q_t is the amount (mg) of CR adsorbed per g of adsorbent (mg g^{-1}) at time t; k_1 (min^{-1}) and k_2 (g mg^{-1} min^{-1}) are the rate constants of pseudo first-order and pseudo second-order adsorption, respectively.

The R^2 and RMSE can be determined by the following equations:

$$R^2 = 1 - \frac{\sum_{n=1}^{n}(q_{e.exp.n} - q_{e.cal.n})^2}{\sum_{n=1}^{n}(q_{e.exp.n} - \overline{q_{e.exp.n}})^2} \qquad \textbf{Eqn. 6}$$

$$RMSE = \sqrt{\frac{1}{n-1}\sum_{n=1}^{n}(q_{e.exp.n} - q_{e.cal.n})^2} \qquad \textbf{Eqn. 7}$$

Nonlinear plots of q_t (mg g^{-1}) versus t (min) for A-OB adsorbent are presented in **Figure 5** and kinetic parameters (k_1, k_2 and q_e) obtained from pseudo-first-order and pseudo second-order equations are summarized in **Table 1**. **Figure 5** shows that, for A-OB adsorbent, there was rapid adsorption for the first 100 min but thereafter slower adsorption was observed. Therefore, the adsorption capacity increases with the increase of contact time and with the increase of the initial concentration until the equilibrium is reached. This behavior can be explained by the fact that all surface binding sites were rapidly filled, and then the CR gradually diffused into the pores of composite beads. The contact time of CR adsorption on A-OB was approximatively 300 min for all initial CR concentrations.

According to the results presented in **Table 1**, the adsorption kinetics for CR on A-OB is better described by the PSO kinetic model because the R^2 values are close to unity, and the RMSE values are lower than those of the PFO model in all initial concentrations, in most cases, respectively. Previous results related to the adsorption kinetics of CR by different alginate-composites also support the pseudo second-order model [12,23].

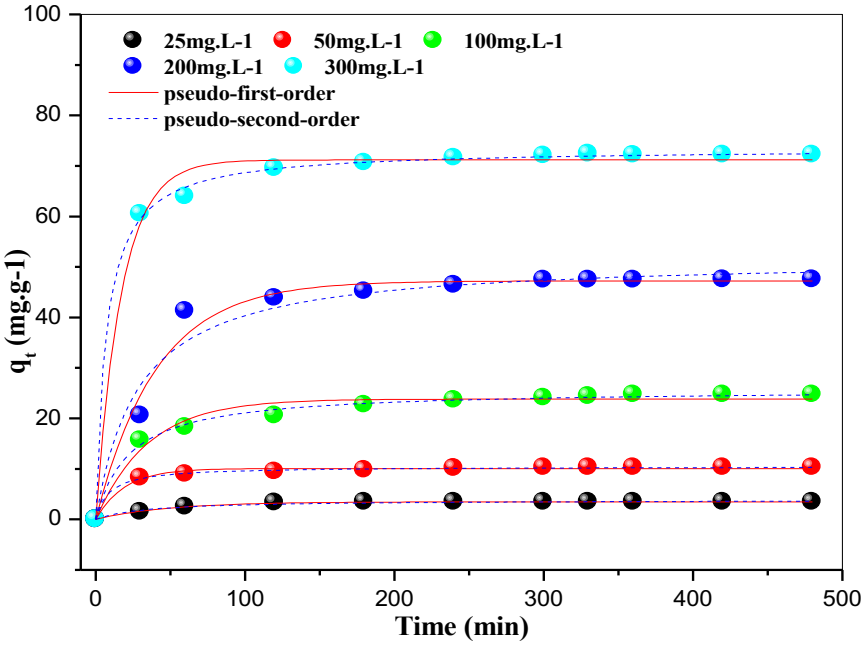

Figure 5. Effect of contact time on the adsorption of CR onto A-OB at different concentrations (m = 100 mg, V = 100 mL, agitation speed = 200 rpm, T= 24 ± 1°C, pH= 7.2)

Table 1. Kinetic parameters for the adsorption of CR onto A-OB composite beads.

C_0 (mg L^{-1})	$q_{e,exp}$ (mg g^{-1})	Pseudo-first-order model, non linear fit				Pseudo-second-order model, non linear fit			
		$q_{e,cal}$	k_1*10^{-3}	R^2	RSME	$q_{e,cal}$	k_2*10^{-3}	R^2	RSME
25	3.46	03.48	20.91	0.995	0.068	3.87	7.49	0.972	0.217
50	10.32	10.07	51.87	0.984	0.346	10.48	10.59	0.997	0.133
100	24.74	23.83	28.67	0.968	1.201	25.80	1.73	0.994	0.468
200	47.49	47.22	24.53	0.979	1.919	51.86	67.56	0.961	2.989
300	72.2	71.18	58.00	0.990	1.813	73.46	1.94	0.998	0.740

C_0 (mg L^{-1}), q_e (mg g^{-1}), k_1 (L min^{-1}), k_2 (g mg^{-1} min^{-1}).

3.4 Adsorption mechanism

In any adsorption study, it was very important to examine the controlling mechanism of adsorption process [40]. The model of the intra-particle diffusion was used in order to determine the phenomenon limiting the mechanism of adsorption. The kinetic data of CR adsorption onto A-OB were fitted to Weber and Morris model, which can be written as follows:

$$q_t = K_i * t^{1/2} + C \qquad \textbf{Eqn. 8}$$

Where k_{id} is the intra-particle diffusion rate constant (mg g^{-1} $min^{-1/2}$); C is the intercept related to the boundary layer effect.

k_{id} can be evaluated from the linear curve of $q_t = f(t^{1/2})$. The values of constants of the diffusion (k_{id}) and coefficients of correlation (R^2) are presented in **Table 2**. When the plot of q_t versus $t^{1/2}$ is linear and passes through the origin, the intra-particle diffusion is the only rate-limiting step, otherwise, if the intercept of plots does not equal zero, then it indicates that the intra-particle diffusion is not the only rate determining step. In order to elucidate which mechanism controls the adsorption kinetics of CR onto A-OB, the diffusion film model has been applied. This model is used to distinguish between the film diffusion and the intraparticle diffusion. Liquid film diffusion model was expressed as follows:

$$-ln\left(1-\frac{q_t}{q_e}\right) = k_{fd}\, t \qquad \textbf{Eqn. 9}$$

Where $F = \frac{q_t}{q_e}$ is the fraction of solute adsorbed and k_{fd} is the liquid film diffusion constant.

In the presence of linear or non-linear plots of -ln(1-F) versus t at different initial concentrations that do not pass through the origin, the adsorption process follows the film diffusion mechanism.

The examination of **Figure 6 (A)** indicates that the curves are not linear over the whole-time range for all concentration levels studied which proof that the intraparticle diffusion is not the mechanism determining of the adsorption into A-OB beads. It exists, but it is done at the same time as the other mechanisms of diffusion [35]. The curves can be separated into two different linear regions. This may reveal that there are two adsorption stages taking place. The first part describes the instant adsorption stage where, CR adsorption rate is high, because of the hydrophobic interactions between the surfactant aggregates and anionic dyes and the low competition between the dye molecules could significantly contribute to the adsorption process [41,42]. The second part describes the slow adsorption stage caused by the low concentration gradients and that finally produced the equilibrium condition. The dye particles from external surface were transferred and adsorbed into the pores of the adsorbent (intraparticle diffusion) [35,43]. The Boyd plots presented in **Figure 6 (B)** are linear, but do not pass through the origin, explaining the influence of film diffusion mechanism on the adsorption rate. In the other hand, by comparing the data presented in **Table 2**, the R^2 values for the film diffusion model are higher than those of intraparticle diffusion model, suggesting that, the film diffusion controls the adsorption rate of CR onto A-OB.

3.4 Isotherm study

Nonlinear isotherms models were applied to study the sorption behavior. The Langmuir and Freundlich models were used for isotherm modeling. Langmuir model assumes that the adsorption phenomenon is in monolayer and under a homogeneous surface. Freundlich model assumes that the multilayer adsorption is done onto the heterogeneous surface. They can be described by the following equations (**Eqn. 10** and **Eqn. 11** respectively):

$$q_e = K_F C_e^{\frac{1}{n}} \qquad \textbf{Eqn. 10}$$

$$q_e = \frac{q_m K_L C_e}{1+K_L C_e} \qquad \textbf{Eqn. 11}$$

Where q_e is the adsorbed amount of dyes per gram of the adsorbent at equilibrium (mg g^{-1}); Ce is the equilibrium concentration of adsorbates (mg L^{-1}); q_m is the maximum monolayer capacity (mg g^{-1}); K_L is the Langmuir isotherm constant (L mg^{-1}); K_F is the Freundlich isotherm constant ((mg g^{-1})(L mg^{-1})$^{1/n}$; n (g L)$^{-1}$ related to the adsorption intensity predicts chemical, physical and linear adsorption system [15].

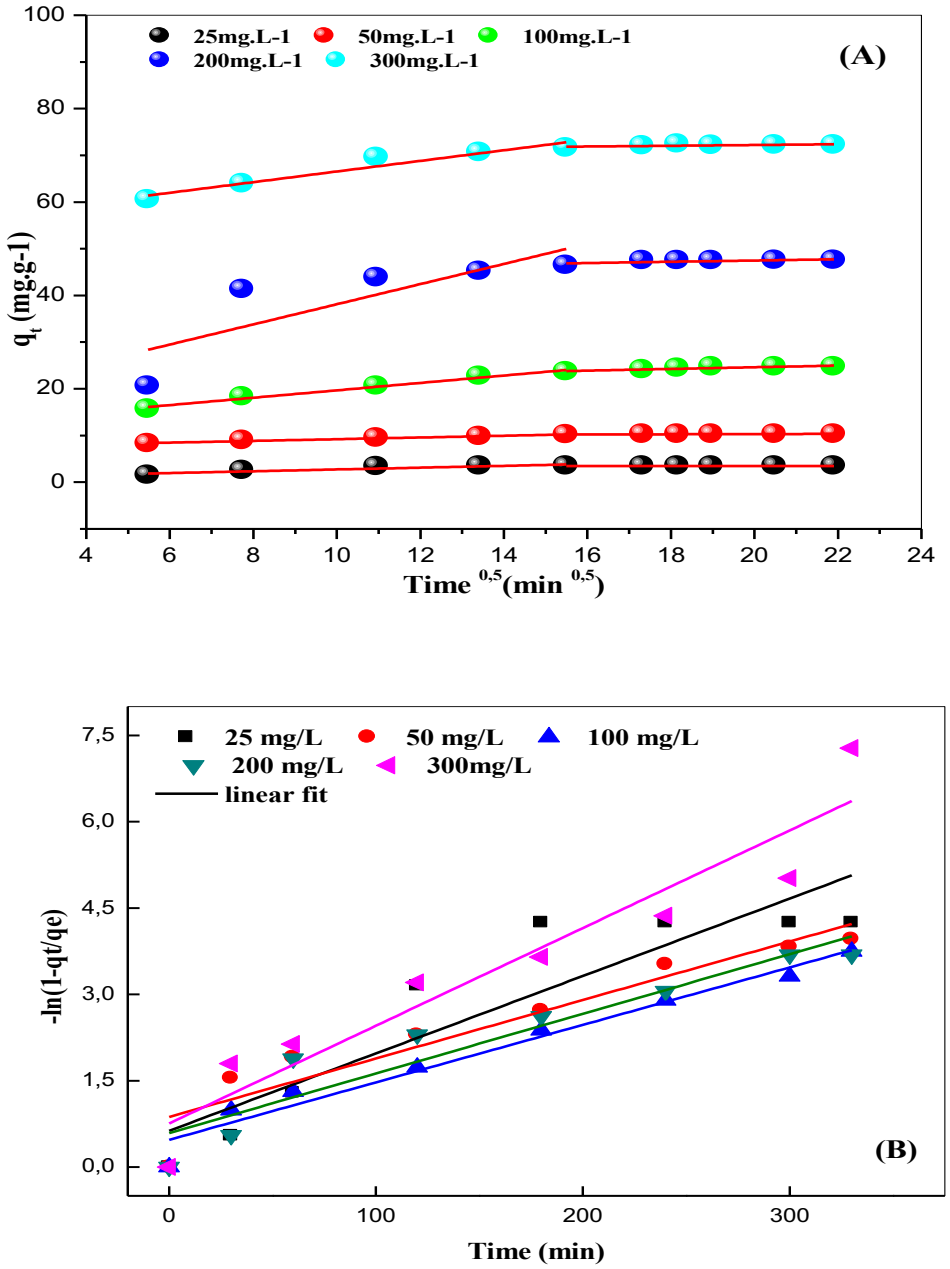

Figure 6. Intraparticle (A) and film diffusion of CR adsorption onto A-OB

Table 2. Intraparticle diffusion and film diffusion parameters in adsorption of CR onto A-OB.

C_0 (mg L^{-1})	Intraparticle diffusion				Film diffusion	
	Step 1		Step 2			
	k_{id}	R^2	k_{id}	R^2	K_{fd}	R^2
25	1.219	0.904	0.024	0.480	0.01345	0.807
50	2.451	0.950	0.116	0.538	0.01016	0.884
100	5.037	0.890	0.107	0.482	0.00999	0.961
200	6.514	0.779	0.111	0.325	0.01036	0.886
300	0.316	0.958	0.009	0.157	0.01697	0.900

Figure 7 shows the nonlinear fits of Langmuir and Freundlich isotherm models of the experimental data. The values of isothermal parameters such as constant terms of the Langmuir (q_m, K_L) and Freundlich (K_F, n) isothermal models, their correlation coefficients (R^2) and their residual root mean square error (RMSE) are summarized in **Table 3**.

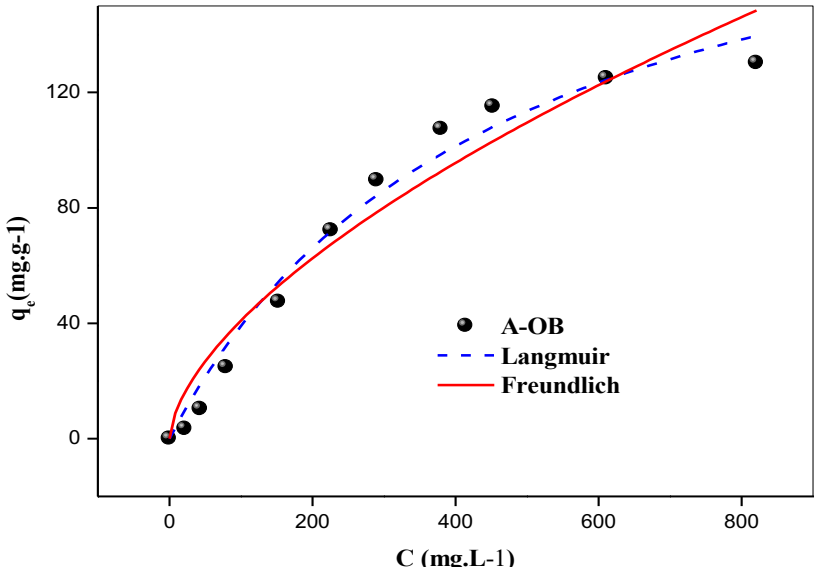

Figure 7. Langmuir and Freundlich isotherms of CR adsorption onto A-OB (C_{CR} = 25-800 mg L^{-1}; m = 100 mg; V = 100 mL; agitation speed = 200 rpm; T = 24±1 °C, pH= 7.2).

The adsorption isotherm of CR on A-OB given in **Figure 7**; shows that was an L-type appearance according to Gilles classification, characterized by a low adsorption capacity. The R^2 and RMSE values were respectively recorded to be 0.98 and 7.13 for Langmuir model and 0.94 and 12.24 for Freundlich model (see **Table 3**). According to the highest correlation coefficient R^2 and the lowest RMSE, CR adsorption onto A-OB is best described by the Langmuir model. This result indicates that adsorption sites of A-OB are uniforms, having the same adsorption energy and a monolayer adsorption takes place.

Table 3. Langmuir and Freundlich isotherm parameters for the adsorption of CR on A-OB.

Models	Parameters	A-OB
Langmuir	**q_m (mg g^{-1})**	217.51
	K_L (L mg^{-1})	0.0021
	R^2	0.980
	RMSE	7.133
Freundlich	**K_F**	2.43
	1/n	1.63
	R^2	0.941
	RMSE	12.242

In addition, K_L values are less than unity (K_L= 0.0021 L mg^{-1}), which indicate the favourability of CR adsorption on A-OB composite beads**.** In the Freundlich model, the slope 1/*n* is a measure of the adsorption intensity or surface heterogeneity where, a value close to zero indicates high heterogeneity, a value of less than 1 indicates a normal Langmuir isotherm, and a value of more than 1 is indicative of

a physical process [44]. In our case 1/n=1.63 is more than 1, it indicates that the adsorption of CR on A-OB is unfavourable and occurs according to homogeneous and physical process [44-46].

We can also use the maximum adsorption capacity (q_m) as a key parameter to evaluate and compare the performance of different adsorbents through the work of the literature. The dye used as adsorbate and the adsorption conditions were taken into account for comparison in the present study. Some previously reported q_m values for the adsorption of Congo red dye by different types of adsorbents are summarized in **Table 4**.

Table 4. Comparison of maximum Congo red adsorption capacity obtained with previous data

Adsorbent	q_m (mg g^{-1})	References
Alginate/Organobentonite beads	217.51	This study
Alginate/bentonite	95.6	[12]
HDTMAB (cationic surfactant) modified clinoptilolite	200.00	[15]
Hydroxyapatite (HAp) /Brij-93 surfactant,	139.0	[46]
Ag_2O–Al_2O_3–ZrO_2/rGO	333.32	[47]
CABI nano-goethite	181.1	[23]
Bentonite/chitosan@cobalt oxide composite	303	[11]
Bent_C12mimCl	158.73	[48]
(Chit/AILP-Kao) nanocomposite	104.6	[35]

3.4 Effect of temperature

The values of thermodynamic parameters such as Gibb's free energy ($\Delta G°$), enthalpy ($\Delta H°$), and entropy ($\Delta S°$) at different temperatures (283, 293, 303, and 313 K) were calculated using **Eqn. 12, 13** and **14**. Changes to $\Delta G°$, $\Delta H°$, and $\Delta S°$ with temperature were calculated to elucidate the process of adsorption [49,50]. According to the laws of thermodynamics, $\Delta G°$ of adsorption is calculated as follows:

$$\Delta G^0 = RTlnK_d \qquad \textbf{Eqn. 12}$$

Where K_d is the distribution coefficient (dimensionless), R is the universal gas constant (8.314 J mol^{-1} K^{-1}), and T is the absolute temperature (K).

The other thermodynamic parameters for adsorption can be calculated via:

$$\Delta G^0 = \Delta H^0 - T\Delta S^0 \qquad \textbf{Eqn. 13}$$

Van't Hoff equation:

$$lnK_d = -\frac{\Delta H^0}{RT} + \frac{\Delta S^0}{R} \qquad \textit{Eqn. 14}$$

The values of $\Delta H°$ and $\Delta S°$ were obtained respectively from the slope and intercept from the plot of $\ln K_d$ versus $1/T$ (see **Figure 8**). The values of $\Delta G°$ were calculated from **Eqn. 13**. **Table 5** shows the calculated values of the thermodynamic parameters $\Delta H°$, $\Delta S°$, and $\Delta G°$.

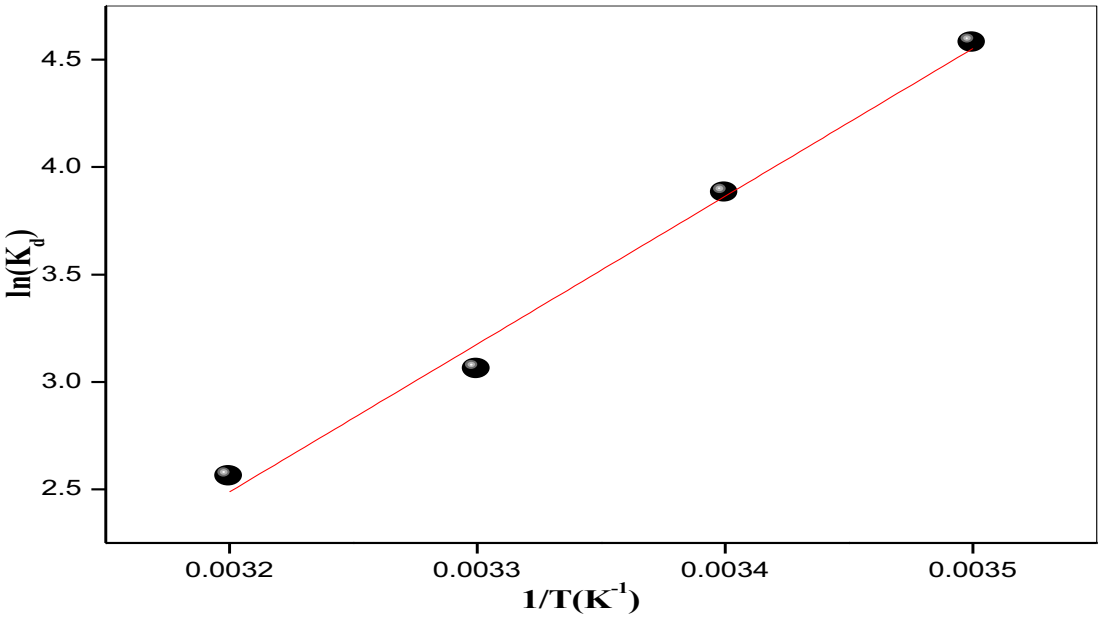

Figure 8. Vant Hoff's plot of the Congo red adsorption by A-OB adsorbent.

The negative value of ΔH° (-57.20 kJ mol^{-1}) indicated that the adsorption process is exothermic and likely to be dominated by physical processes in nature involving weak forces of attraction [51,52]. Negative value of ΔS° (-162.35 kJ mol^{-1} K^{-1}) indicates that the randomness at the solution/adsorbent interface has decreased during the adsorption process, and no significant changes occur in the internal structure of the adsorbents by the adsorption of CR on A-OB composite beads [50,51]. The values of ΔG° at all applied temperatures (283–313 K) are negatives indicating that the reaction processes are spontaneous, and the more negative reflecting a more energetically favorable process [53,54].

Table 5: Thermodynamic parameters for Congo red adsorption onto A-OB

T (K)	ΔG° (kJ mol^{-1})	ΔH° (kJ mol^{-1})	ΔS° (kJ mol^{-1} K^{-1})
283	-11.25		
293	-9.63	-57.20	-162.35
303	-8.00		
313	-6.38		

In addition, the negative value increases with the decrease of temperature (see **Table 5**) suggesting the feasibility of the process, that adsorption is spontaneous and is more favorable at lower temperatures [15,53]. This may be attributed to the greater mobility of the dye molecules in the solution at lower temperatures, which improves their adsorption at the adsorbent surface. Additionally, the ΔG° values provide insight into the nature of the adsorption process (chemisorption is associated with ΔG° values ranging from −80 to −400 kJ mol^{-1}, and physisorption with ΔG° values ranging from −20 to 0 kJ mol^{-1}) [23]. The ΔG° values for CR adsorption on A–OB composite beads were in the range of −11.25 to −6.38 kJ mol^{-1}. Hence, this process can be considered as physisorption.

3.4 Regeneration study

The regeneration of adsorbent is a significant economic factor for the treatment process. Regeneration cycles are shown in **Figure 9**.

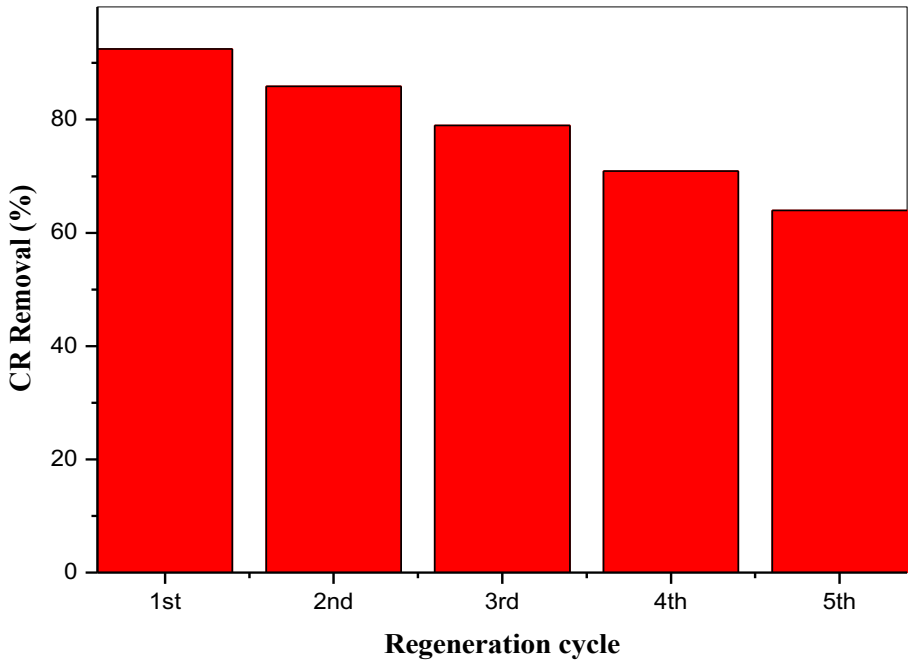

Figure 9. The results of regeneration test for the adsorption of CR onto A-OB composite beads.

In the first cycle of adsorption-desorption, the regeneration shows a performance of 92.5%, then, the adsorption-desorption percentage was decreased intensively by the increase of the cycles number (up to 5). The percentage (%) of CR removal varies in the following order (from the first to the fifth cycle respectively): 92.5, 85.88, 78.96, 70.93 and 63.96%. The same results were also observed by certain authors [12,28, 29,54].

Conclusion

Adsorbent prepared from organobentonite entrapped in calcium alginate A-OB was used to remove an anionic dye of Congo red (CR) from aqueous phase in batch system. It was found that the prepared composite can effectively remove Congo red (CR) anionic dye. Among the evaluated isotherms, Langmuir was found to be the best fitted isotherm model with higher R^2 and lower RMSE value. The maximum monolayer capacity of adsorption (q_m) was found to be 217.51 mg g^{-1}. The adsorption kinetics was well described by the pseudo-second-order model. CR adsorption process was found to be spontaneous and exothermic. As the prepared composite beads are no pollutant, very effective, biodegradable and low-cost, we can suggest that these adsorbents could be utilized for the treatment of anionic dyes from industrial wastewaters.

References

1. A. Ghaffar, G. A. Shar, M. A. Tahir, M. Iqbal, M. Abbas, M. Adil, S. Ehtisham-ul-Haque, B. Munir, M. Yameen, Vibrio fischeri bioluminescence inhibition assay for ecotoxicity assessment: a review, *Sci. Total Environ.* 626 (2018) 1295–1309. doi.org/10.1016/j.scitotenv.2018.01.066

2. Y. Aoulad El Hadj Ali, A. D. N'diaye, D. Fahmi, M. Sid'Ahmed Kankou, M. Stitou. Adsorption of Congo red from aqueous solution using *Typha australis* leaves as a low cost adsorbent, *J. Environ. Treat. Tech.* 9 (2021) 534-539. https://doi.org/10.47277/JETT/9(2)539
3. M. C. Collivignarelli, A. Abbàb, M. C. Miino, S. Damiani, Treatments for color removal from wastewater: state of the art, *J. Environ. Manag.* 236 (2019) 727–745. https://doi.org/10.1016/j.jenvman.2018.11.094
4. A. D N'diaye, Y. Aoulad El Hadj Ali, O. El Moustapha Abdallahi, M. A. Bollahi, M. Stitou, M. Kankou, D. Fahmi, Sorption of Malachite Green from aqueous solution using *Typha australis* leaves as a low cost sorbent, *J. Environ. Treat. Tech.* 8(3) (2020) 1023-1028.
5. R. Novikau , G. Lujaniene, Adsorption behaviour of pollutants: Heavy metals, radionuclides, organic pollutants, on clays and their minerals (raw, modified and treated): A review, *J. Environ. Manag.* 309 (2022) 114685. https://doi.org/10.1016/j.jenvman.2022.114685
6. A. D. N'diaye, Y. Aoulad El Hadj Ali, M. A. Bollahi, M. Stitou, M. S. A. Kankou, D. Fahmi, Adsorption of Methylene Blue from aqueous solution using Senegal River *Typha australis*, *Mediterr. J. Chem.* 10 (2020) 22-32. http://dx.doi.org/10.13171/mjc10102001221185adn
7. Y. Aoulad El Hadj Ali, M. Ahrouch, A. Ait Lahcen, A. D. N'diaye, F. El Yousfi, M. Stitou, Dried sewage sludge as an efficient adsorbent for pollutants: cationic methylene blue removal case study, *Nanotechnol. Environ. Eng.* 6 (2021) Article 17. https://doi.org/10.1007/s41204-021-00111-6
8. A. Oussalah, A. Boukerroui, Alginate-bentonite beads for efficient adsorption of methylene blue dye, *Euro. Mediterr. J. Environ. Integr.* 5 (2020) Article 31. https://doi.org/10.1007/s41207-020-00165-z
9. D. Aberkane, C. Meziti, S. Ihaddaden, A. Boukerroui, B. Cagnon, Calcium alginate-regenerated spent bleaching earth composite beads for efficient removal of methylene blue, *Can. J. Chem. Eng.* 100 (2022) 1001-1012. doi: 10.1002/cjce.24217
10. A. Kausar, M. Iqbal , A. Javed, K. Aftab, Z. H. Nazli, H. N. Bhatti, S. Nouren, Dyes adsorption using clay and modified clay: a review, *J. Mol. Liq.* 256 (2018) 395-407. https://doi.org/10.1016/j.molliq.2018.02.034
11. M. R. Abu Khadra, A. Adlii, B. M. Bakry, Green fabrication of bentonite/chitosan@cobalt oxide composite (BE/CH@Co) of enhanced adsorption and advanced oxidation removal of congo red dye and Cr (VI) from water, *Int. J. Biol. Macromol.* 126 (2019) 402–413. https://doi.org/10.1016/j.ijbiomac.2018.12.225
12. A. Oussalah, A. Boukerroui, A. Aichour, B. Djellouli, Cationic and anionic dyes removal by low-cost hybrid alginate/natural bentonite composite beads: adsorption and reusability studies, *Int. J. Biol. Macromol.* 124 (2019) 854–862. https://doi.org/10.1016/j.ijbio mac.2018.11.197
13. M. Toor, B. Jin, S. Dai , V. Vimonses, Activating natural bentonite as a cost-effective adsorbent for removal of Congo red in wastewater, *J. Ind. Eng. Chem.* 21 (2015) 653-661. http://dx.doi.org/10.1016/j.jiec.2014.03.033
14. R. Ples¸ Chicinas¸ H. Bedelean, R. Stefan , A. Maicaneanu, Ability of a montmorillonitic clay to interact with cationic and anionic dyes in aqueous solutions, *J. Mol. Struct.* 1154 (2018) 187-195. https://doi.org/10.1016/j.molstruc.2017.10.038
15. R. Nodehi, H. Shayesteh, A. R. Kelishami, Enhanced adsorption of congo red using cationic surfactant functionalized zeolite particles, *Microchem. J.* 153 (2020) 104281. https://doi.org/10.1016/j.microc.2019.104281

16. W. Li, Q. Ma, Y. Bai, D. Xu, M. Wu, H. Ma, Facile fabrication of gelatin/bentonite composite beads for tunable removal of anionic and cationic dyes, *Chem. Eng. Res. Des.* 134 (2018) 336-346. https://doi.org/10.1016/j.cherd.2018.04.016
17. E. Saavedra-Labastida, M. C. Díaz-Nava, J. Illescas, C. Mur, Comparison of the removal of an anionic dye from aqueous solutions by adsorption with organically modified clays and their composites, *Water Air Soil Pollut.* 230 (88) (2019) 1-26. https://doi.org/10.1007/s11270-019-4131-z
18. L.B. de Paiva, A. R. Morales, F. R. Valenzuela Díaz, Organoclays: properties, preparation and applications, *Appl. Clay Sci.* 42 (2008) 8-24. doi:10.1016/j.clay.2008.02.006
19. F. Ayari , G. Manai, S. Khelifi, M. Trabelsi-Ayadi, Treatment of anionic dye aqueous solution using Ti, HDTMA and Al/Fe pillared bentonite. Essay to regenerate the adsorbent, *J. Saudi Chem. Soc.* 23 (2019) 294-306. https://doi.org/10.1016/j.jscs.2018.08.001
20. S. Pandey, A comprehensive review on recent developments in bentonite-based materials used as adsorbents for wastewater treatment, *J. Mol. Liq.* 241 (2017) 1091-1113. http://dx.doi.org/10.1016/j.molliq.2017.06.115
21. B. Wang, Y. Wan, Y. Zheng, X. Lee, T. Liu, Z.Yu, J. Huang, Y. S. Ok, J. Chen, B. Gao, Alginate-based composites for environmental applications: a critical review, *Crit. Rev. Env. Sci. Tec.* 49 (2019) 318-356. https://doi.org/10.1080/10643389.2018.1547621
22. A. Oussalah, A. Boukerroui, Removal of cationic dye using alginate–organobentonite composite beads, *Euro. Mediterr. J. Environ. Integr.* 5 (2020) Article 55. https://doi.org/10.1007/s41207-020-00199-3
23. V. S. Munagapati, D.S. Kim, Equilibrium isotherms, kinetics, and thermodynamics studies for Congo red adsorption using calcium alginate beads impregnated with nano-goethite, *Ecotoxicol. Environ. Saf.* 141 (2017) 226-234. DOI: 10.1016/j.ecoenv.2017.03.036
24. A. Oussalah Caractérisation et modification d'une argile de Maghnia: applications, Doctorate thesis, University of Bejaia (2020) Bejaia (Algeria).
25. A. Besq, C. Malfoy, A. Pantet, P. Monnet, D. Righi, Physicochemical characterisation and flow properties of some bentonite muds, *Appl. Clay Sci.* 23 (2003) 275-286. https://doi.org/10.1016/S0169-1317(03)00127-3
26. B. Makhoukhi, M. Djab, M.A. Didi, Adsorption of Telon dyes onto bis-imidazolium modifed bentonite in aqueous solutions, *J. Environ. Chem. Eng.* 3 (2015) 1384-1392. https://doi.org/10.1016/j. jece.2014.12.012
27. A. Boukerroui, M.S. Ouali, Activation d'une bentonite par un sel d'ammonium: évolution de la capacité d'échange et de la surface spécifque, *Ann. Chim. Sci. Mat.* 25 (2000) 583-590
28. N. Belhouchat, H. Zaghouane-Boudiaf, C. Viseras, Removal of anionic and cationic dyes from aqueous solution with activated organo-bentonite/sodium alginate encapsulated beads, *Appl. Clay Sci*. 135 (2017) 9-15. https://doi.org/10.1016/j.clay.2016.08.031
29. Y. He, Z. Wu, L. Tu, Y. Han, G. Zhang, C. Li, Encapsulation and characterization of slow-release microbial fertilizer from the composites of bentonite and alginate, *Appl. Clay Sci.* 109-110 (2015) 68-75. https://doi.org/10.1016/j.clay.2015.02.001
30. A. Aichour, H. Zaghouane-Boudiaf, C.V. Iborra, M.S. Polo, Bioadsorbent beads prepared from activated biomass/alginate for enhanced removal of cationic dye from water medium: kinetics, equilibrium and thermodynamic studies, *J. Mol. Liq.* 256 (2018) 533-540. https://doi.org/10.1016/j.molliq.2018.02.073

31. N. Djebri, M. Boutahala, N. Chelalia, N. Boukhalfa, L. Zeroual, Enhanced removal of cationic dye by calcium alginate/organobentonite beads: modeling, kinetics, equilibriums, thermodynamic and reusability studies, *Int. J. Biol. Macromol.* 92 (2016) 1277-1287. https ://doi.org/10.1016/j.ijbiomac.2016.08.013
32. R.R. Pawar, G.P. Lalhmunsiama, S.Y. Sawant, B. Shahmoradi, S.M. Lee, Porous synthetic hectorite clay alginate composite beads for effective adsorption of methylene blue dye from aqueous solution, *Int. J. Biol. Macromol.* 114 (2018) 1315-1324. https://doi. org/10.1016/j.ijbiomac.2018.04.008
33. M.K. Purkait, A. Maiti, S. Das Gupta , S. De, Removal of Congo red using activated carbon and its regeneration, *J. Hazard. Mater.* 145 (2007) 287-295. doi:10.1016/j.jhazmat.2006.11.021
34. A. Aichour, H. Zaghouane-Boudiaf, Synthesis and characterization of hybrid activated bentonite/alginate composite to improve its effective elimination of dyes stuff from wastewater. *Appl. Water Sci.* 10 (2020). https://doi.org/10.1007/s13201-020-01232-0
35. R. Ahmad, K. Ansari, Comparative study for adsorption of Congo red and methylene blue dye on chitosan modified hybrid nanocomposite, *Process Biochem.* 108 (2021) 90-102. https://doi.org/10.1016/j.procbio.2021.05.013
36. R. Ahmad, A. Mirza, Green synthesis of Xanthan gum/Methionine-bentonite nano composite for sequestering toxic anionic dye, *Surf. Interfaces* 8 (2017) 65-72. http://dx.doi.org/10.1016/j.surfin.2017.05.001
37. D. Pathania, A. Sharma, Z.-M. Siddiqi, Removal of Congo red dye from aqueous system using Phoenix dactylifera seeds, *J. Mol. Liq.* 219 (2016) 359-367. http://dx.doi.org/10.1016/j.molliq.2016.03.020
38. M. A. Adebayo , J. I. Adebomi, T. O. Abe, F. I. Areo, Removal of aqueous Congo red and malachite green using ackee apple seed–bentonite composite, *Colloids Interface Sci. Commun*. 38 (2020) 100311. https://doi.org/10.1016/j.colcom.2020.100311
39-Tadele Assefa Aragaw, Adugna Nigatu Alene, A comparative study of acidic, basic, and reactive dyes adsorption from aqueous solution onto kaolin adsorbent: Effect of operating parameters, isotherms, kinetics, and thermodynamics, *Emerg. Contam.* 8 (2022) 59-74. https://doi.org/10.1016/j.emcon.2022.01.002
40. D. Garg, C.B. Majumder, S. Kumar, B. Sarkar, Removal of Direct Blue-86 dye from aqueous solution using alginate encapsulated activated carbon (PnsAC-alginate) prepared from waste peanut shell, *J. Environ. Chem. Eng.* 7 (2019) 103365. https://doi.org/10.1016/j.jece.2019.103365
41. T.S. Anirudhan, M. Ramachandran, Adsorptive removal of basic dyes from aqueous solutions by surfactant modified bentonite clay (organoclay): kinetic and competitive adsorption isotherm. *Process Saf. Environ. Prot.* 95 (2015) 215-225. http://dx.doi.org/10.1016/j.psep.2015.03.003
42. L. Zhu, L. Wang, Y. Xu, Chitosan and surfactant co-modified montmorillonite: a multifunctional adsorbent for contaminant removal, *Appl. Clay Sci.* 146 (2017) 35-42. http://dx.doi.org/10.1016/j.clay.2017.05.027
43. Y. Li, Q. Du, T. Liu, X. Peng, J. Wang, J. Sun, Y. Wang, S. Wu, Z. Wang, Y. Xia, L. Xia, Comparative study of methylene blue dye adsorption onto activated carbon, graphene oxide, and carbon nanotubes, *Chem. Eng. Res. Des.* 91 (2013) 361-368. DOI: 10.1016/j.cherd.2012.07.007
44. G.O. El-Sayed, Removal of methylene blue and crystal violet from aqueous solutions by palm kernel fiber, *Desalination* 272 (2011) 225-232. doi:10.1016/j.desal.2011.01.025

45. T. Benhalima, H. Ferfera-Harrar, Eco-friendly porous carboxymethyl cellulose/dextran sulfate composite beads as reusable and efficient adsorbents of cationic dye methylene blue, *Int. J. Biol. Macromol.* 132 (2019) 126-141. https://doi.org/10.1016/j.ijbiomac.2019.03.164
46. H. Bensalah, S. A. Younssi, M. Ouammou, A. Gurlo, M. F. Bekheet, Azo dye adsorption on an industrial waste-transformed hydroxyapatite adsorbent: kinetics, isotherms, mechanism and regeneration studies, *J. Environ. Chem. Eng.* 8 (2020) 103807. https://doi.org/10.1016/j.jece.2020.103807
47. G. Sharma, T. S. AlGarni, P. S. Kumar, S. Bhogal, A.Kumar, S. Sharma, M. Naushad, Z. A. ALOthman, F. J. Stadler Utilization of Ag_2O–Al_2O_3–ZrO_2 decorated onto rGO as adsorbent for the removal of Congo red from aqueous solution, *Environ. Res.* 197 (2021) 111179. https://doi.org/10.1016/j.envres.2021.111179
48. R. Ozola-Davidane, J. Burlakovs, T. Tamm, S. Zeltkalne, A. E. Krauklis, M. Klavins, Bentonite-ionic liquid composites for Congo red removal from aqueous solutions, *J. Mol. Liq.* 337 (2021) 116373. https://doi.org/10.1016/j.molliq.2021.116373
49. E.C. Lima, A.H. Bandegharaei, J.C. Moreno-Piraján, I. Anastopoulos A critical review of the estimation of the thermodynamic parameters on adsorption equilibria. Wrong use of equilibrium constant in the Van't Hoof equation for calculation of thermodynamic parameters of adsorption, *J. Mol. Liq.* 273 (2019) 425-434. https:// doi.org/10.1016/j.molliq.2018.10.048
50. Y. Liu, Is the free energy change of adsorption correctly calculated? *J. Chem. Eng. Data* 54 (2009) 1981-1985. https://doi.org/10.1021/ je800661q
51. V. Vimonses, S. Lei, B. Jin, C. W.K. Chow, C. Saint, Kinetic study and equilibrium isotherm analysis of congo red adsorption by clay materials, *Chem. Eng. J.* 148 (2009) 354-364. doi:10.1016/j.cej.2008.09.009
52. M. Maqbool, S. Sadaf, H. N. Bhatti, S. Rehmat , A. Kausar , S. A. Alissa , M. Iqbal, Sodium alginate and polypyrrole composites with algal dead biomass for the adsorption of congo red dye: kinetics, thermodynamics and desorption studies, *Surf. Interfaces* 25 (2021) 101183. https://doi.org/10.1016/j.surfin.2021.101183
53. M. Mondal, K. Sinha, K. Aikat, G. Halder, Adsorption thermodynamics and kinetics of ranitidine hydrochloride onto superheated steam activated carbon derived from mung bean husk, *J. Environ. Chem. Eng.* 3 (2015) 187-195. https://doi.org/10.1016/j.jece.2014.11.021
54. F. Ding, M.Gao , T. Shen, H. Zeng, Y. Xiang, Comparative study of organo-vermiculite, organo-montmorillonite and organo-silica nanosheets functionalized by an ether-spacer-containing Gemini surfactant: congo red adsorption and wettability, *Chem. Eng. J.* 349 (2018) 388-396. https://doi.org/10.1016/j.cej.2018.05.095